TRAJECTORY OPTIONS FOR LOW-COST MISSIONS TO EASILY RETRIEVABLE OBJECTS

Dong Qiao,* Colin R. McInnes†

Near-Earth Objects (NEOs) are of contemporary interest, since asteroids and comets hold the key clues to understanding the origin of the solar system and the formation of the planets, and also have a speculated wealth of material resources. The exploitation of these resources has been discussed as a means to lower the cost of future space endeavours. Recently, a new family of so-called Easily Retrievable Objects that can be transported from accessible heliocentric orbits into the Earth's neighbourhood at affordable costs, have been presented. In this paper, the trajectory options for low-cost missions to EROs are explored. We consider a wide variety of multi-impulse transfer and gravity-assist transfer with mid-course maneuvers to obtain low launch energy rendezvous trajectories to EROs. There trajectories are constructed by analytic and numerical search methods, and hybrid optimization algorithms including global search and local search to find the optimal rendezvous opportunities. The best rendezvous opportunities for currently known EROs in the next 20 years are reported. The relevant mission costs are analyzed. A discussion of general characteristics of the various trajectory types is presented.

INTRODUCTION

Asteroids and comets hold key clue to understanding the formation, evolution and composition of the solar system. Among asteroid and comet populations, Near-Earth asteroids are of particular interest because of their accessibility from Earth, but also their speculated wealth of material resources. Near-Earth asteroids are usually divided into four classes, depending upon their orbital characteristics: Atens, Apollos, Amors and Atiras. Atens and Apollos are Earth-crossers. Orbits of Amors and Atiras are completely outside and inside the orbit of the Earth, respectively.

Recently, a new family of so-called Easily Retrievable Objects (EROs) [1] was presented. EROs are defined as objects that can be gravitationally captured in bound periodic orbits around the collinear libration points L_1 and L_2 of the Sun-Earth system under a certain Δv threshold, arbitrarily selected for this work at 500m/s. These objects include 2006 RH120, 2010VQ98, 2007 UN12, 2010UE51, 2008EA9, 2011UD21, 2009BD, 2008UA202, 2011BL45, 2011MD, 2000SG344

* Associate Professor, School of Aerospace Engineering, Beijing Institute of Technology, Beijing, 100081, China.
† Professor, Advanced Space Concepts Laboratory, University of Strathclyde, Glasgow, G1 1XQ, UK.

and 1991VG. The EROs with capture costs and types are listed in Table 1. Orbital elements of EROs are listed in Table 2.

In this work, we focus on outbound trajectories and opportunities to EROs. The capture phase is not considered here. The multi-impulse transfer and gravity-assist transfer with mid-course maneuvers are considered to lower launch energy and total velocity increments. A hybrid optimization approach including global search and local search is used to find the low-cost transfer trajectories. The general characteristics of the various trajectory types are discussed.

Table 1. NEO Characteristics for Transfer Trajectories with $\Delta\upsilon$ Below 500m/s.

Asteroid name	MOID (AU)	Diameter (m)	$\Delta\upsilon$ (km/s)/capture type
2006 RH120	0.0171	2.3-7.4	0.058/2Hs; 0.107/2Hn; 0.187/2V; 0.298/2P
2010 VQ98	0.0048	4.3-13.6	0.181/2V; 0.393/2Hn; 0.487/2Hs;
2007 UN12	0.0011	3.4-10.6	0.199/2P; 0.271/2Hs; 0.327/2Hn; 0.434/2V
2010 UE51	0.0084	4.1-12.9	0.249/2Hs; 0.340/2P; 0.470/2V; 0.474/2Hn
2008 EA9	0.0014	5.6-16.9	0.328/2P;
2011 UD21	0.0043	3.8-12.0	0.356/1Hs; 0.421/1V; 0.436/1Hn
2009 BD	0.0053	4.2-13.4	0.392/2Hn; 0.487/2V
2008 UA202	0.0003	2.4-7.7	0.393/2Hn; 0.425/2P; 0.467/2Hs
2011 BL45	0.0040	6.9-22.0	0.400/2V
2011 MD	0.0018	4.6-14.4	0.422/2V
2000 SG344	0.0008	20.7-65.5	0.443/1P; 0.449/1Hs; 0.468/1Hn
1991 VG	0.0037	3.9-12.5	0.465/2Hs; 0.466/2V;

Note: the type of transfer is indicated by a 1 or 2 indicating L1 or L2 plus the letter for Planar Lyapunov, V for vertical Lyapunov, and Hn or Hs for north and south halo.

Table 2. Orbital Elements of EROs.

Asteroid name	Major semi-axis, a (AU)	Eccentricity, e	Inclination, i (deg.)	Longitude of ascending node, Ω (deg.)	Ascending node-perihelion angle, ω (deg.)	Mean anomaly, M (deg.)	Orbital elements at Epoch

2006 RH120*	1.033244	0.024486	0.024486	51.14552	10.18774	315.0344	2456300. 5
2010 VQ98	1.023149	0.027066	1.475927	46.16582	341.6317	337.6236	2456600.5
2007 UN12	1.053742	0.060481	0.235263	216.1032	134.3419	242.7026	2456600.5
2010 UE51	1.055239	0.059680	0.624412	32.28553	47.22822	243.0871	2456600.5
2008 EA9	1.059135	0.079834	0.424560	129.4679	335.8608	123.9744	2456600.5
2011 UD21	0.978817	0.030367	1.062538	22.35797	209.6922	190.6708	2456600.5
2009 BD*	1.061719	0.051550	1.267116	253.3269	316.7272	205.2121	2456300. 5
2008 UA202	1.033317	0.068708	0.264245	21.05432	300.8913	345.4208	2456600.5
2011 BL45	1.037850	0.020999	3.049076	134.7844	155.1223	62.16631	2456600.5
2011 MD	1.056318	0.037099	2.445655	271.6291	5.941064	59.42011	2456600.5
2000 SG344	0.977526	0.066918	0.111267	192.0956	275.1380	108.0862	2456600.5
1991 VG	1.027016	0.049178	1.445459	73.97961	24.55356	358.9310	2456600.5

Note. * The orbital elements of 2006RH120 and 2009BD come from http://smallbodies.ru/. Others take from JPL solar system dynamics http://ssd.jpl.nasa.gov/sbdb.cgi.

MISSION MODELING AND TRAJECTORY OPTIMIZATION

Mission Assumptions

It is assumed that a spacecraft departs from a low-altitude circular parking orbit above the Earth for an interplanetary trip to an asteroid. The primary mission design consideration for a rendezvous is usually the velocity increment budget. This is some function of the velocity increments needed at the point of departure to insert the spacecraft into the transfer trajectory, and the change required to cancel the relative velocity between spacecraft and target at arrival. Since the orbital properties of EROs are similar to that of Earth, the relative phase angle between target asteroids and the Earth becomes the important factor to influence on the total velocity increment or launch energy. A midcourse impulse or planetary gravity-assist will be used to reduce it.

During the outbound transfer, the departure velocity increment accounts for a large proportion of fuel consumption. It assumes that the spacecraft escapes from a 200km-altitude circular parking orbit above the Earth. The relation between departure velocity increment $\Delta \upsilon_L$ and hyperbolic excess velocity υ_∞ is shown in Figure 1.

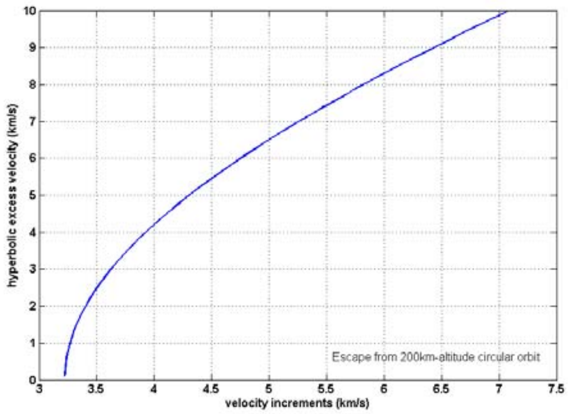

Figure 1. Relation between departure velocity increment and hyperbolic excess velocity (200km-altitude circular parking orbit).

As shown in Figure 1, when the hyperbolic excess velocity υ_∞ is about 1km/s, the departure velocity increment $\Delta\upsilon_L$ is about 3.2697km/s. If the υ_∞ increases to 3km/s, namely the launch energy C_3 is equal to 9km^2/s^2, the departure velocity increment $\Delta\upsilon_L$ will be 3.6258km/s, while if υ_∞ reaches 4 km/s, the $\Delta\upsilon_L$ is also close to 4km/s, about 3.9286km/s. It is worth noting that the minimum hyperbolic excess velocity υ_∞ for a transfer from Earth to Venus is more than 2 km/s, but less than 3km/s. For the Mars, the minimum hyperbolic excess velocity υ_∞ will be more than 3km/s, but less than 4km/s. This is an important observation for designing the interplanetary mission. If the hyperbolic excess velocity for a transfer directly from Earth to an asteroid is less than 3 km/s, Venus or the Mars will not be considered as the gravity-assist body.

If the parking orbit is elliptic, the departure velocity increment will closely related to the semi-major axis of the parking orbit. It is assumed that the perigee of the parking orbit is 200km altitude above Earth. The relation between departure velocity increment, hyperbolic excess velocity and apogee of parking orbit is shown in Figure 2.

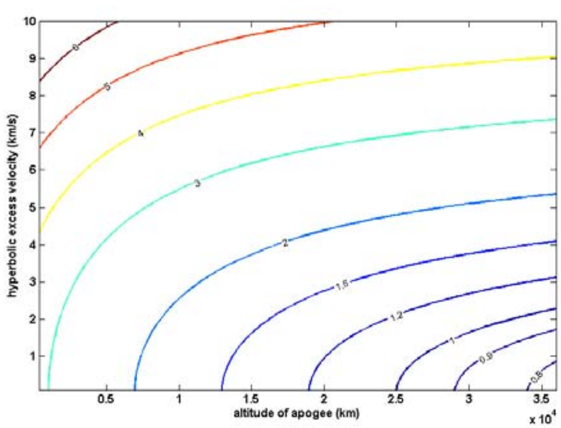

Figure 2. Relation between departure velocity increment, hyperbolic excess velocity and apogee of parking orbit

As can be seen in Figure 2, the departure velocity increment will reduce as the altitude of apogee increases. Compared with the 200km-altitude circular parking orbit, the required velocity increments for departure from GTO with an altitude of perigee and apogee of 200km and 35000km, yields a 2.5km/s decrease, when the hyperbolic excess velocity is about 1km/s. If the hyperbolic excess velocity reaches 3 km/s, the departure velocity increment from GTO grows from 0.8 km/s to 1.2km/s.

The analysis assumes that a chemical rocket engine is used and the initial mass of the spacecraft is 5000kg. According to Tsiolkovsky's rocket equation, the fuel consumption can then be evaluated. For the different specific impulses, the relation between velocity increment and remaining mass of the spacecraft is shown in Figure 3.

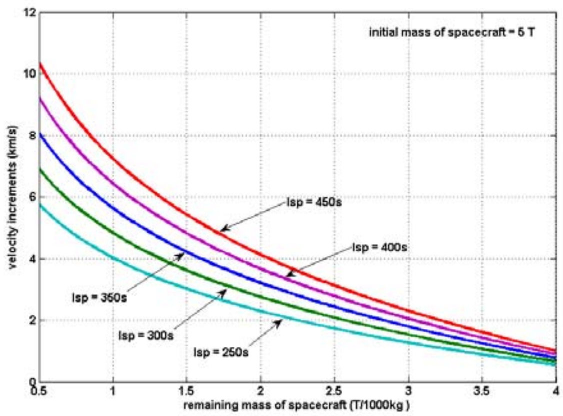

Figure 3. Relation between velocity increment and remaining mass

As shown in Figure 3, if a rocket engine with specific impulse of 250s is used, 4000kg of fuel is required to deliver 4.0km/s of velocity increment. If it's assumed that a specific impulse of 450s is selected, 4.0km/s of velocity increment needs about 3000kg of fuel. The specific impulse of bi-propellant liquid rockets can be up to 450s. Of course, if the ion thruster is selected, the situation will change, but will not be discussed here.

Trajectory Optimization

To the rendezvous with EROs, the procedure searches for the trajectory that satisfies the rendezvous condition, while minimizing the characteristic velocity, which is the performance index:

$$J = \Delta\upsilon_{total} = \Delta\upsilon_L + \sum_i \Delta\upsilon_{mi} + \Delta\upsilon_a$$

The characteristic velocity $\Delta\upsilon_{total}$ is the sum of the velocity changes that are performed by expending the propellant where $\Delta\upsilon_L$ is the velocity increments required to leave the Earth parking orbit and travel along a heliocentric transfer trajectory to reach the target asteroid. It is obtained from:

$$\Delta\upsilon_L = \sqrt{(\boldsymbol{\upsilon}_L - \boldsymbol{\upsilon}_E)^2 + \upsilon_e^2} - \upsilon_{Ep}$$

where $\boldsymbol{\upsilon}_E(t)$ and $\boldsymbol{\upsilon}_L(t)$ are the velocity vector of Earth and spacecraft around the Sun, respectively and υ_e and υ_{Ep} are the magnitudes of the Earth-relative escape and actual velocities, respectively, at the perigee. In addition $\Delta\upsilon_{mi}$ is the midcourse impulse, where the contribution of midcourse burns to the characteristic velocity is related only to the change of the Sun-relative velocity such that:

$$\Delta\upsilon_{mi} = \sqrt{(\boldsymbol{\upsilon}_{mi+} - \boldsymbol{\upsilon}_{mi-})^2}$$

Lastly, $\Delta\upsilon_a$ is the velocity increment required to rendezvous with target asteroid. Neglecting the asteroid gravity, we can estimate the rendezvous impulse as follows:

$$\Delta\upsilon_a = \sqrt{(\boldsymbol{\upsilon}_a - \boldsymbol{\upsilon}_T)^2}$$

where $\boldsymbol{\upsilon}_T(t)$ and $\boldsymbol{\upsilon}_a(t)$ is the velocity vector of target asteroid and spacecraft around the Sun.

In this paper, a hybrid optimization approach is used to search for optimal transfer opportunities. In the hybrid optimization approach, the differential evolution (DE) algorithm[2] serves as a starter engine that identifies regions of global minima within the trajectory solution space. Then the best candidate of the DE algorithm parameter population is submitted as an initial parameter set to a sequential quadratic programming[3] (SQP) module for refinement.

TWO-IMPULSE DIRECT TRANSFER

According to the above model and approach, the optimal two-impulse rendezvous opportunities for currently known EROs in the 2015-2035 years are shown in Figure 4a and 4b.

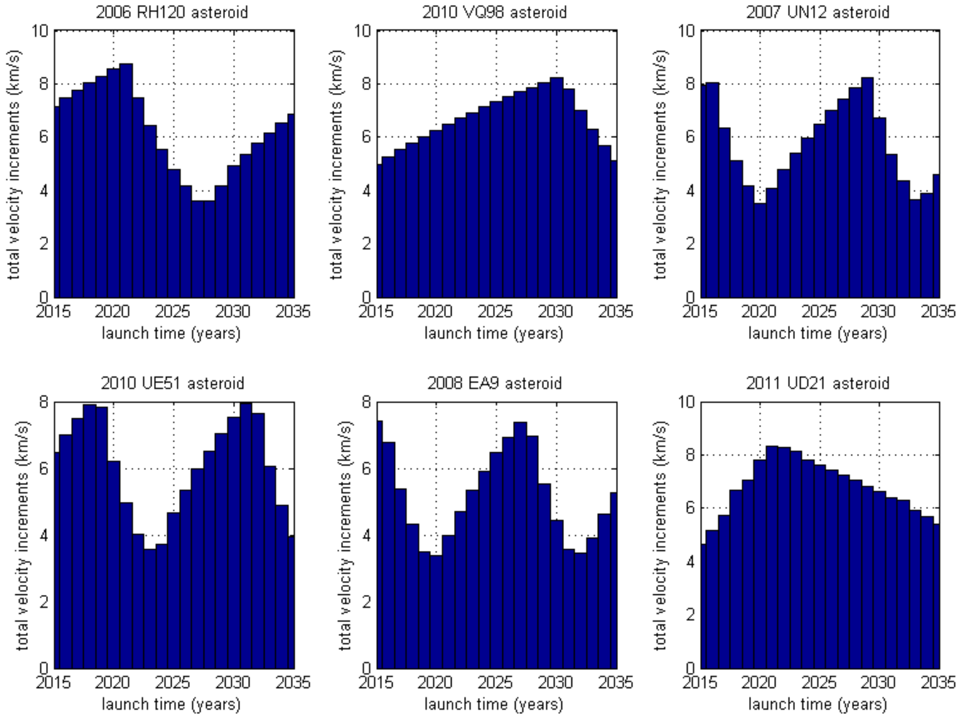

Figure 4a. The optimal two-impulse rendezvous opportunities for EROs in the 2015-2035 years

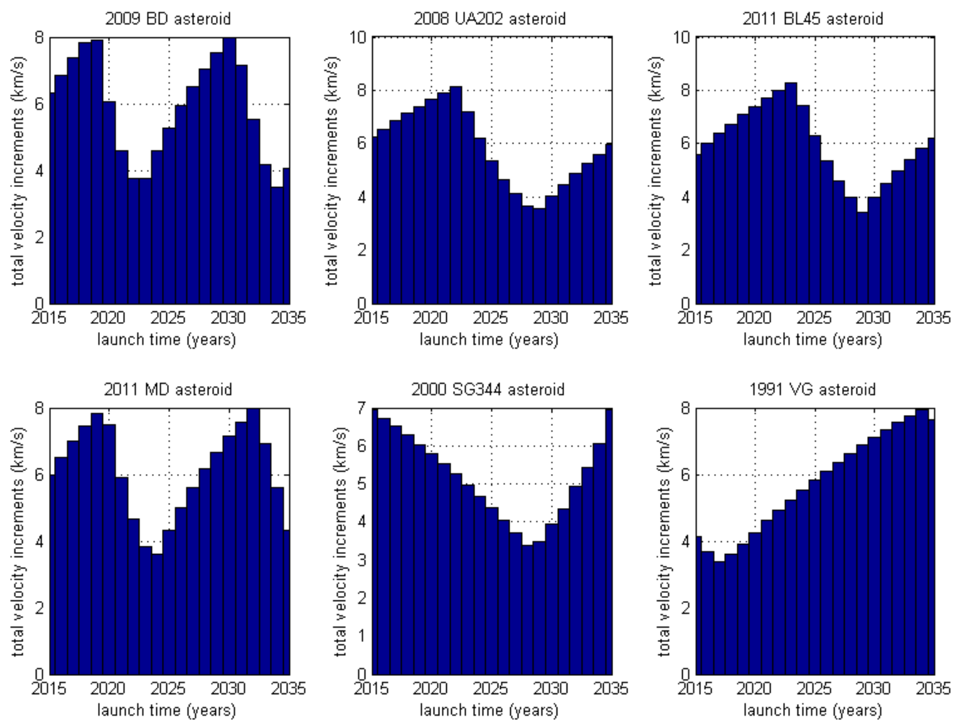

Figure 4b. The optimal two-impulse rendezvous opportunities for EROs in the 2015-2035 years

As shown in Figure 4a and 4b, the maximum total velocity increment of the optimal two-impulse rendezvous opportunities for all of currently known EROs in the 2015-2035 years is about 8.76km/s, where the corresponding object is 2006 RH120 and launch date is about 2021. The maximum total velocity increment for the optimal two-impulse opportunities for 2010UE51, 2008EA9, 2009BD, 2011MD, 2000SG344, 1991VG, are less than 8.0 km/s. At the same time, the minimum total velocity increment for the optimal two-impulse opportunities for all of EROs in the 2015-2035 is about 3.37km/s, corresponding to asteroid 2000SG344 with a launch date of 2028. The minimum total velocity increment of all of EROs is less than 4.0km/s except 2010VQ98 and 2011UD21.

From the Figure 4a and 4b, we also can see that the rendezvous opportunities show quasi-periodicities. In the 2015-2035 timespan, the quasi-periodicities are found for the following three cases: one rendezvous period (such as 2006 RH120, 2008 UA202 and 2011 BL45), more than one period (2007 UN12, 2010 UE51, 2008 EA9, 2009 BD and 2011 MD), and less than one period (2010 VQ98, 2011 UD21, 2000 SG344 and 1991 VG). The main reason for the emergence of quasi-periodic phenomenon is the periodic changes of relative phase angle of the Earth and asteroid. These periodic changes are also reflected in the transfer orbit.

For the above three cases, we choose 2006 RH120, 2007 UN12 and 2010 VQ98 as examples to analyze transfer trajectories and trajectory parameters. In the one-period case, according to the velocity increment and flight time, the transfer trajectories can be divided into three families. These transfer families are shown in Figure 5.

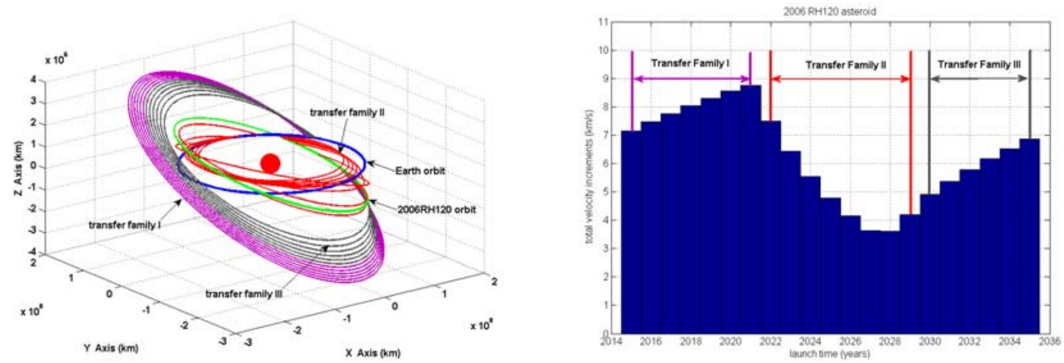

Figure 5. The transfer families and corresponding parameters for 2006 RH120 asteroid

As can be seen from Figure 5, transfer family I requires a larger velocity increment and longer flight times than others. It also implies that the relative phase angle between Earth and 2006 RH120 in this timeframe are not suitable for mission design. The transfer family II, compared with transfer family I, needs a shorter flight time and lower velocity increment. From Figure 5, we also can see that the transfer trajectories of low-cost opportunities get close to the orbit of 2006 RH120, such as flight paths in 2027 and 2028. For family III, the required velocity increment and flight time grow.

For the more-than-one-period case, we take 2007 UN12 as an example. On basis of the velocity increment and flight time, the two transfer families are found. The corresponding flight paths and trajectory parameters are shown in Figure 6.

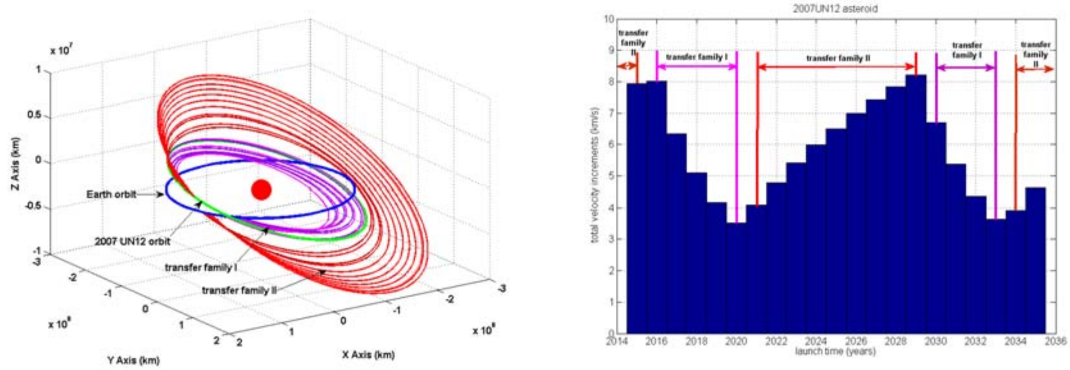

Figure 6. The transfer families and corresponding parameters for 2007 UN12 asteroid

As shown in Figure 6, the flight paths of transfer family I are located inside the orbit of 2007 UN12, and that of transfer family II are of outside. In the transfer family I, with time passing, the required velocity increment will decrease and the flight path will close to the 2007 UN12 asteroid's orbit. However, in the transfer family II, it is quite the reverse.

For the less-than-one-period case, the transfer trajectories are obviously divided into two transfer families. For example, for 2010 VQ98, the flight paths and trajectory parameters are shown in Figure 7.

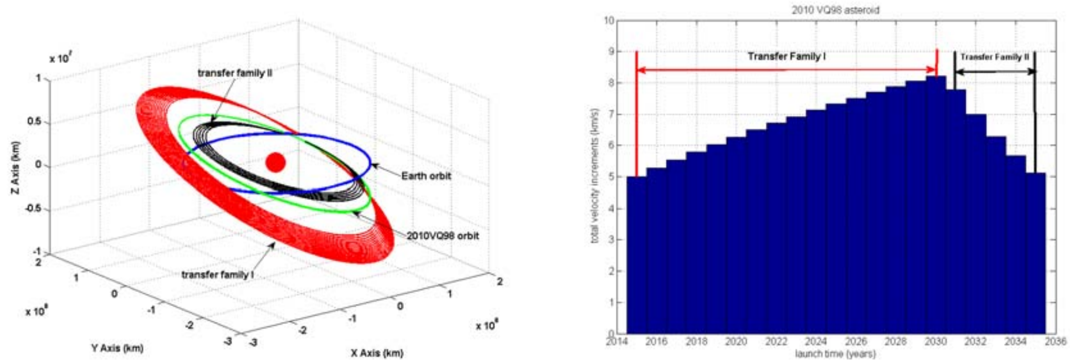

Figure 7. The transfer families and corresponding parameters for 2010 VQ98 asteroid

As can be seen in Figure 7, there is similar phenomenon. For the transfer family I case, flight times and velocity increments of transfer trajectories grow. The flight paths will also extend outward and be away from the orbit of 2010 VQ98. The transfer family II case will be quite the reverse.

MULTI-IMPULSE TRANSFER

Multi-impulse transfer is one of important transfer types for interplanetary missions. In this section, the three-impulse transfer and four-impulse transfer will be considered. These midcourse impulses are mainly used to adjust the orbit phase angle and reduce the velocity increment. Comparisons of optimal two-impulse and multi-impulse transfer for EROs in the 2015-2035 years are shown in Figure 8a, 8b and 8c.

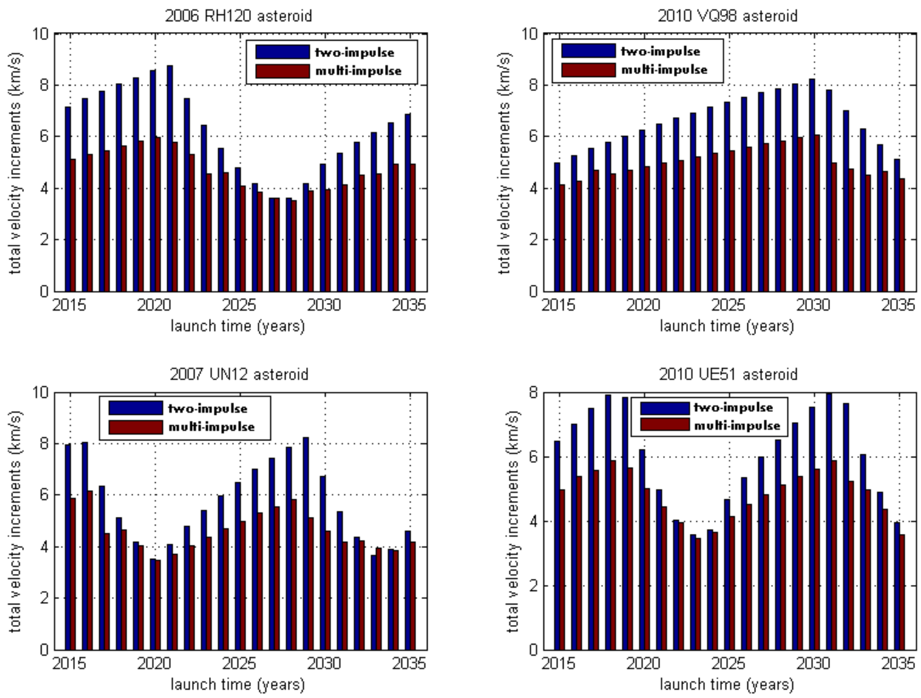

Figure 8a. Comparison of two- and multi-impulse transfer for EROs in the 2015-2035 years

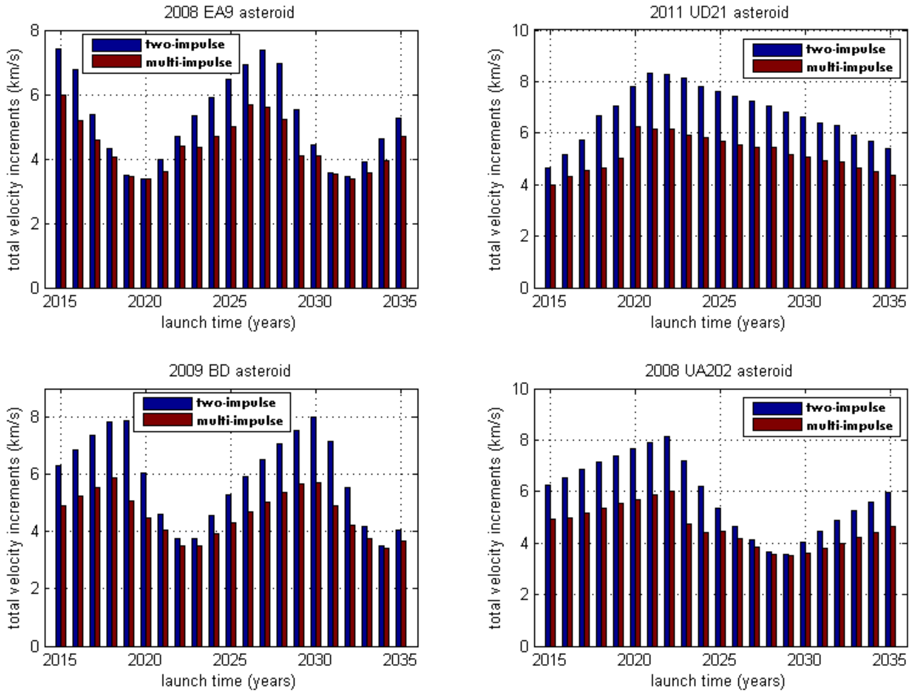

Figure 8b. Comparison of two- and multi-impulse transfer for EROs in the 2015-2035 years

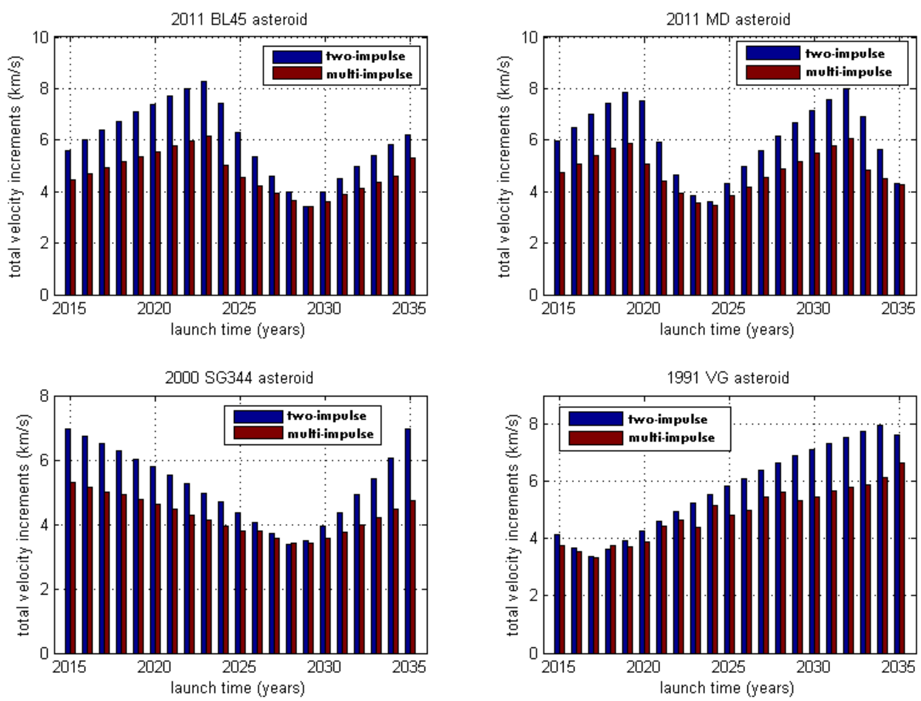

Figure 8c. Comparison of two- and multi-impulse transfer for EROs in the 2015-2035 years

As shown in Figure 8a, 8b and 8c, compared with optimal two-impulse transfer, the total velocity increments of optimal multi-impulse transfer, especially of the maximum total velocity increment, are obviously reduced. The maximum total velocity increment of all optimal multi-impulse transfers for EROs in the 2015-2035 years is about 6.64km/s, corresponding to 1991 VG with a launch date about 2035. All of the maximum total velocity increments of optimal multi-impulse transfer opportunities for EROs are less than 6.20 km/s, except 1991 VG. This is a significant observation because the 6.0km/s of velocity increment can be reached by using bi-propellant liquid rockets on the basis of the above evaluation. At the same time, we also can find that although there is little change in velocity increment over time, rendezvous quasi-periodicities still remain.

GRAVITY-ASSIST TRANSFER

The gravity-assist technique is an effective approach to reduce launch energy and total velocity increment in interplanetary missions. In this paper, considering the orbital characteristic of EROs is similar to the Earth's orbit, we select the Earth as the gravity-assist body. So the transfer strategy of the Earth gravity assist with deep-space maneuver (ΔV-EGA) will be used. The gravity-assist strategy can be simply described as follows: a spacecraft is launched from Earth into a heliocentric orbit with a period slightly greater or smaller than an integer number of years. At aphelion or perihelion, a deep-space maneuver is applied to lower the perihelion or raise the aphelion to intercept nontangentially the Earth with hyperbolic excess velocity higher than that at launch. The deep-space maneuver enables the Earth to be used as a gravity-assist body to increase or decrease the heliocentric energy of the spacecraft. The types of ΔV-EGA transfer orbit are manifold and can be found in the literature[4] and so will not be reviewed here.

According to the above calculations and analysis, 2006 RH120, 2010 VQ98, 2011 UD21 and 1991 VG are selected as the targets to use the ΔV-EGA transfer to reduce the velocity increment further. We don't use the gravity-assist strategy for all of EROs, because some rendezvous opportunities with the optimal two-impulse or multi-impulse have shown lower velocity increments. The gravity-assist strategy can reduce the velocity increment, but increase the flight time. The compromise between fuel consumption and flight time is considered. Comparisons with optimal two-impulse, multi-impulse transfer and gravity assist of 2006 RH120, 2010 VQ98, 2011 UD21 and 1991 VG in different years are shown in Figure 9 .

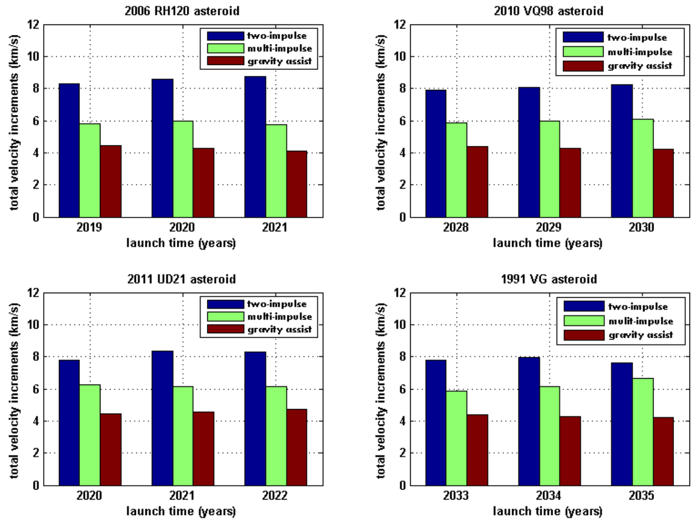

Figure 9 Comparison of two-, multi-impulse transfer and gravity-assist transfer for some EROs

As shown in Figure 9, the total velocity increment of the ΔV-EGA transfer, compared with the maximum total velocity increment of the optimal two-impulse transfer of 2006 RH120 asteroid in 2021, can reduced the total velocity increment by 4.63km/s. Compared with the maximum total velocity increments of the optimal multi-impulse transfer of 1991 VG in 2035, the ΔV-EGA transfer has a 2.41km/s decrease in velocity increment. At the same time, we also can see that all of the total velocity increments of selected targets in the corresponding timeframe are less then 4.70km/s. These targets appear reasonably accessible.

CONCLUSION

In this paper, we focus on the rendezvous opportunities to EROs in the timeframe 2015-2035. The low-cost transfer trajectories are found by using optimal two-impulse, multi-impulse and ΔV-EGA transfer methods. According to the above analysis, the total velocity increment of all of the currently known EROs can be reduced to 5.50km/s or less. The best opportunities, such as 2000 SG344, are less than 3.40km/s.

For some targets, longer low-cost rendezvous periods are found. For example, the best rendezvous periods of 2006 RH120 and 2008 UA202 remain for 6 years, from 2025 to 2030 and from 2027 to 2032, respectively. During that period, the total velocity increment is less then 4.0 km/s. For 2000 SG344, the best rendezvous period remains for 9 years, namely starting from 2024 and ending in 2032.

Some targets also show stable requirements of velocity increments. For example, the total velocity increments of 2010 VQ98 and 2011 UD21 are more than 4.0 km/s and less than 6.0 km/s. For 2007 UN12, 2010 UE51, 2008 EA9, 2009 BD, 2011 BL45, 2011 MD and 1991 VG, the total velocity increments have larger changes. The higher velocity increments are close to 6.0 km/s and the lower can reach as low as 3.50km/s. If the gravity-assist transfer applies for every target, the maximum total velocity increments will be expected to reduce to about 5.0km/s.

ACKNOWLEDGMENTS

The work was supported by the program for New Century Excellent Talents in University (NCET), Beijing Higher Education Young Elite Teacher Project and supported by China Scholarship Council.

REFERENCE

[1] D.Garc?a Y?arnoz, J.P. Sanchez and C.R.McInnes, "Easily Retrievable Objects among the NEO Population." *Celestial Mechanics and Dynamical Astronomy*. Vol. 116, No.4, 2013, pp. 367–388.

[2] R. Stom and K. Price, "DE a Simple and Efficient heuristic for Global Optimization over Continuous Space." *Journal of Global Optimization*. Vol. 11, No.4, 1997, pp. 41–359.

[3] P.T. Boggs and J.W. Tolle, "Sequential Quadratic Programming." *Acta Numerica* . Vol. 4, No.4, 1995, pp. 1–51.

[4] J.A. Sims, J.M. Longuski and A.J.Staugler, "Vinf Leveraging for Interplanetary Missions: Multiple Revolution Orbit Techniques." *Journal of Guidance, Control and Dynamics*. Vol. 20, No. 3, 1997, pp.409–415.